Hydrogeochemical investigation of the groundwater of Curaçao

Iris Verstappen

MSc thesis

May 2022

Supervisors: Victor Bense and Martine van der Ploeg

Mike Wit and Boris van Breukelen

Hydrology and Quantitative Water Management Group

Wageningen University and TU Delft

Abstract

The health of Curaçao's coral reefs is declining: a coral cover decrease of 50% since 1980, stresses the urge to investigate the cause. However, little is known about which processes are the main stressors for this deterioration on Curaçao. Therefore, a large research project, SEALINK, has been set-up to assess how land-derived and waterborne inputs effect the corals. By sampling ground-, rain- and treated waste water, this study gives insight into the current groundwater quality and the changes compared to previous research (1977 and 1992) as a first step in investigating how groundwater affects the health of the coral reef. All samples were collected in the rainy season of 2021; in total 22 physical, chemical and a biological parameters were determined and analysed with the use of chemical ratios, Piper diagram and a Principle Component Analysis (PCA). Interpretation of analytical data show that salinisation, cation exchange, chemical weathering and pollution are influencing the groundwater chemistry, coming forward in PCA too. The groundwater of Curaçao can be used for irrigation, however, it is not suitable as drinking water. Data shows that cesspits and septic tank effluents are causing a decrease in groundwater pH over time, and that seawater intrusion is increasingly influences the groundwater quality in the Knip and Midden formation. In the prospective of further research, it is important to evaluate the measured concentrations on their possibility to harm coral reefs and based on those outcomes to zoom in, and set-up a denser sampling network and find out where the groundwater reaches the ocean as submarine groundwater discharge.

Contents

Chapter 1

Introduction

1.1 Problem description

Worldwide, the health of coral reefs is rapidly declining. The coral reefs are threatened by a list of factors, among others, natural phenomena and anthropogenic factors such as a growing human population, tourism and contamination (Jager, 2019). The coral reefs of Curaçao are face this problem as well. Even though the coral reefs around Curaçao are regarded as the healthiest of the Caribbean, they have suffered an alarming decrease of 50% in coral cover between 1980 and 2015 (Estep, Sandin, & Vermeij, 2017). With coral reefs being of major importance for the biodiversity, economy (tourism and fishery) and coastal defence by breaking the waves, this is a decline to be concerned about (Waitt, 2016).

One natural phenomenon influencing the coral reefs' health and functioning is the input of fresh water, whether or not polluted along the way. After intense rain events, surface runoff is a pathway for nutrients, sediments and contaminants to reach the sea. Compared to the other Caribbean islands, Curaçao has little topography and a lack of year-round rainfall, resulting in a relative small amount of runoff. The Waitt Institute (2017) assumes that this low runoff input is the reason for Curaçao's "healthy coral" compared to the other Caribbean islands. Another pathway for fresh water to reach the ocean is the so called submarine groundwater discharge (SGD). This continuous up-welling groundwater from the seabed could be a pathway for nutrients and pollutants to end up in the ocean (Estep et al., 2017). Because there is little known about this process on Curaçao, there is little knowledge about its effect on Curaçao coral reefs. Also the relative proportion of it compared to runoff is underexamined (Vermeij, 2019).

Another threat for the reefs of Curaçao is the direct source of pollution caused by wastewater. Only one-third of the households were connected to the sewage system in 2017. The majority of households is connected to septic tanks and cesspits. When not managed properly, these are a potential source of pollution to the groundwater and ocean (Estep et al., 2017). Adding to that, the sewage treatment plants are poorly maintained and do not meet the demands, with as consequence that only 16% of Curaçao's wastewater was purified in 2017. The remaining 84% is discharged untreated into the ocean or the terrestrial environment (Adshead et al., 2018; Jager, 2019). This wastewater discharge is a direct source of pollution and feeds contaminants and an excessive amount of nutrients into the ocean.

Furthermore, it is unknown what the influence of land and water use is on the coral reef health. For example, two large scale groundwater use changes are the stop of groundwater exploitation by the water authority and Shell, who stopped pumping in 1962 and 1973, respectively (Abtmaier, 1978). The water authority started using desalinized seawater for drinking water instead. Nowadays, groundwater is only used for irrigation in combination with treated wastewater. The latter being an extra fresh water input into the system. Besides these factors, a growing population and low maintenance caused a decrease in the number of functional dams, resulting in more surface runoff (Van Buurt, 2018). All these changes cause a shift in the water balance, impacting the hydrogeological situation and the chemical composition of groundwater. Combined, all these previous mentioned factors directly and indirectly influence the water quality on and around the island.

Previous research on Curaçao zoomed in on geological surveys, chemical analyses of wells and springs, as well as on coral reef health and functioning. In 1977/78 Abtmaier performed an extensive hydrogeological survey over the whole island. He measured the transmissivity of all geological formations, compiled water balances for all catchments, performed hydro-chemical investigations and analysed the data.

In 1992 a follow-up groundwater survey was performed by Louws et al. (1997) in 96 wells, 53 overlapping wells. Compared to 1977/78 it was found that 35% of the wells became more saline, presumably caused by saltwater intrusion through over-exploitation of the groundwater. On the other hand, 45% of the wells showed decreasing chloride concentrations. This freshening of the groundwater

could be explained by dilution, caused by irrigation and the leakage of sewage water (Louws, Vriend, & Frapporti, 1997).

In 2000, Sambeek and Eggenkamp performed a groundwater analysis of all wells from the 1992 survey. They found multiple geochemical processes influencing the cat- and anion concentrations of the groundwater. Furthermore, at that time nitrate levels were already found to be above the European drinking-water standard (50 mg/L), caused by polluted (waste) water (Van Sambeek, Eggenkamp, & Vissers, 2000). This level is a major concern, while corals can deal with a maximum concentration of only 2 mg N/L (Jager, 2019).

It is unknown by which pathway and to what extent the land-derived and waterborne inputs are the cause of the decreasing coral health around the island. Above all, it is unknown what the current hydrogeochemical state of the groundwater is (Estep et al., 2017). Hence, a large research program has been set up, called SEALINK. An interdisciplinary team of researchers will investigate which processes affect the growth and survival of coral reef in the Dutch Caribbean. Furthermore, they will investigate which factor is mostly contributing to it and what can be done about it to diminish its influences (Vermeij, 2019).

This master thesis research will contribute to the project by collecting and analysing up-to-date information of the hydrogeochemical situation of the wells, boreholes and water bodies on Curaçao. Next to this, the present situation will be compared with previous research to get insight into the changes in groundwater quality.

1.2 Aim and Objective

The aim of this research is to give an indication about the current hydrogeochemical status of the island. The data collected in 1977 and 1992 will also be used to investigate if the trend in EC found by Louws et al. continued and whether there are other trends over the years. In this way the effects of groundwater quality (changes) on coral reef health can be analysed. This will be accomplished by field measurements and collecting water samples for lab analyses.

1.3 Research questions

The main research question is as follows:

What explains the hydrogeochemical status of Curaçao's groundwater?

Subquestions that will be covered are:

- What is the effect of geology on the groundwater characteristics?
- What effects do anthropogenic processes (land use, sewage system, landfills) have on the groundwater quality?
- What is the hydrogeochemical trend compared to the measurement from 1997 and 1992?

1.4 Thesis outline

Chapter 2 contains the description of the study area. Chapter 3 describes the material and methods used in this study. This section is divided in tree parts: the first part describes the sampling and analytical procedures, the second part explains the performed data analysis, and the third part explains the trend analyse. This is followed by the results (chapter 4) where there is being looked at the spatial variation of the measured variables over the island, the relation between the measured variables to investigate the chemical processes and the change over the years. In the discussion (chapter 5) these results of the spatial variation and chemical relations will be explained based on geo-chemical processes, salinisation and anthropogenic influences. The last chapters comprises the conclusion (chapter 6) and the acknowledgments (chapter 7).

Chapter 2

Study area

2.1 Field site

The island of Curaçao is located in the Dutch Caribbean, north of the coast of Venezuela, see figure 2.1. The island is 444 km2, which can be roughly divided in 3 parts: the western, middle and eastern part, as seen in figure 2.1a. The western part of the island is poorly populated. A large part comprises the Christoffelpark National Park. The highest point of the island is to be found in this nature conserve, the Christoffelberg (372 m). The middle part, is sparsely populated with as main cities Sint Willibrordus, Terra Korá and Grote Berg. Furthermore, landfill Malpais, the waste dump, is located in this part of the island. The east part of the island consist of Willemstad, which is the densely populated capitol of Curaçao, and an inaccessible, privately owned area on the east point.

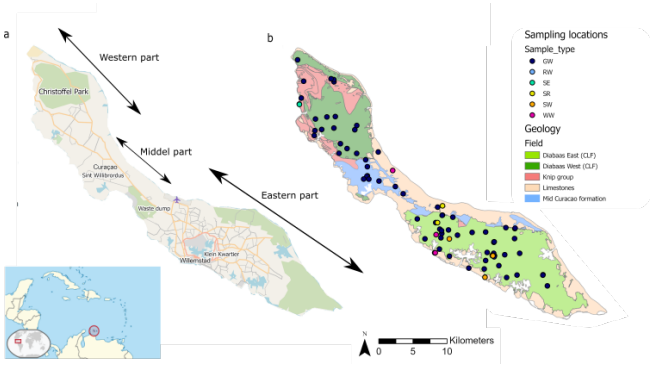

Figure 2.1: Topographic (a) and the geological map of Curaçao with sample locations; GW = groundwater, RW = rain water, SE = seawater, SR = surface runoff, SW = surface water and WW = waste water (b)

2.2 Climate

Curaçao experiences a semi-arid to arid climate with a yearly averaged temperature of 28 °C and 602 mm of rainfall. Most of the rain precipitates during the rainy season (September -January). Important to keep in mind is that the weather on Curaçao is influenced by the El Niño-Southern Oscillation. La Niña will bring more rain and the weather event El Niño a drier year (Martis, Van Oldenborgh, & Burgers, 2002). The average evaporation is 6.9 mm/d, 2500 mm/year (department of Curacao, n.d.). It is assumed that groundwater recharge only occurs during large precipitation events and it is estimated to be 3.5% of the precipitation a year (Abtmaier, 1978).

2.3 Hydrogeology

Curaçao's geology consists of 4 geological units, see figure 2.1b, and is well described by Molengraaf (1929), Abtmaier (1978) and Grontmij and Sogreah,(1968). The Curaçao lava formation (CLF), an igneous rock cooled under the sea surface, is rich in calcium and magnesium. In the rest of the report, the CLF is divided in to two parts: Diabaas West (DW) and Diabaas East (DO). The Knip formation (K) is a higly non-homogeneous formation and mostly consists of sedimentary rocks including mainly silica-rich rocks and clastic sediments (de Vries, 2000). The Midden Curaçao Formation (M) is a mix of sandstone, shale, clay lenses and fine grained conglomerate consisting of carbonate sediments, quarts sediments and basalt. The island is bordered by the highly permeable limestone formations (L). The Knip, Midden and Limestone formation are sedimentary deposits, deposited under sea level and thus rich in marine deposits. It is expected that the groundwater flow is predominantly in the weathered zone and highly influenced by fracture flow.

The groundwater is investigated by Abtmaier (1978), Louws et al. (1997) and Van Sambeek et al. (2000) of samples taken in 1977 and 1992, respectively. The groundwater is rather brackish and some parts of the island (Knip and Midden formation) are assumed to be influenced by remnants of seawater in the geological formations (Louws et al., 1997). Ungoing salinisation processes are seawater intrusion, seaspray and evaporation. Cation concentrations are influenced through cation exchange with the soil surface. Additionally, calcite dissolution, silicate weathering, potassium fixation and pollu-

tion were important processes influencing the groundwater chemistry in 1992 (Van Sambeek et al., 2000).

2.4 Water use

Fresh water is expensive on the island while it is desalinized seawater (Aqualectra, n.d.), this is the reason for most citizens to install a well in their garden. Citizens use the groundwater for irrigation, laundry, the shower and flushing the toilet. Water is being pumped with the use of windmills or electrical pumps. The government has no insight in the construction of wells nor in the exploitation of the wells. Currently, wells are constructed by private well companies with a diameter of 25 cm with an inner PVC casing. Some of the tubes being fully perforated, while others are only open at the well bottom, with as third option that the PVC tube only stabilize the weathered surface layer. These wells will be referred to as boreholes, see appendix figure A.1a for an example.

Dating from the time of the plantations, there are wells with a diameter of $>$2 m. These wells are hand-dug and are provided with concrete to a depth up to hard rock, see appendix figure A.1b. When both hand-dug and boreholes are considered, wells is used.

On the island there are some large dams and hundreds of small dams to capture and store surface runoff in the rain season. The small dams are more efficient in water retention and groundwater recharge, with their smaller surface area they are less subjected to evaporation, consequently, more water can infiltrate into the soil. As mentioned before the dams are poorly maintained, with a drastic decrease of small dams from more than 1500 to around 800 (Van Buurt, 2018).

Only one third of the households is connected to the sewage system (Jager, 2019). The sewage water is being treated in "Klein Hofje" (62%), "Klein Kwartier" (34%). Waste water treatment plant "Abatoir" (1%) is not in use anymore and there is a malfunctioning treatment plant by Tera Kòrá (3%) (Adshead et al., 2018; Erdogan, 2021). Treated waste water of Klein Kwartier is being used by hotels, golf courses and agriculture for irrigation. The treated water of Klein Kwartier infiltrates into the ground by a system of successive infiltration ponds.

Chapter 3

Material and method

In this section the material and methods of the data sampling and analytical procedures (3.1) and data analysis are explained. The methods related to the data analysis are divided in multiple sections. The first section being the data validation methods (3.2), the second section the data analysis of 2021 (3.3) and the third section the trend analysis with 1977 and 1997 (3.4).

3.1 Sampling & analytical procedures

The sampling strategy was designed to obtain spatial variability over the island as well as within the geological formations, as seen in figure 2.1. Furthermore, to not over represent a certain formation in the data, it was aimed to have, in percentage terms, an equivalent amount of samples per formation in relation to the total coverage of that formation. This setup is similar to the surveys performed earlier as seen in appendix table A.1.

In total there are 77 groundwater samples on 70 locations taken and 2 spring samples. In the the CLF are 58 samples collected, 44 on the east of the island (DO) and 14 in the west of the island (DW). In the sedimentary formations 18 samples are collected, of which 7 in the Knip formation (K) , 3 in the limestone formation (L) and 11 in the Midden formation (M), as also mentioned appendix table A.1. Furthermore, some rain, surface runoff, waste water, surface water and sea samples were collected. The locations of all samples can be seen in figure 2.1 and a map of the groundwater sample locations with sample code is seen in appendix figure A.2.

Well measurements were carried out in the period from 25th October to 23th December 2021. The sampling depth was set to 1 m above the bottom of the well to not disturb the sediments nor have a high impact of surface processes. The samples were collected with the use of a bailer and when possible a peristalic pump was used. Sometimes, there has been made use of the pump installed by the owner of the well, with or without a pressure vessel present. The groundwater level and well depth were measured with a Heron Dipper to which an extra weight was attached. For each depth, the dipper directly displayed the EC value, giving an indication about whether there was stratification in the well or not.

In the field Electrical Conductivity (EC), pH, Dissolved Oxygen (DO), redox (pE) and temperature (T) where measured with the Ponsel ODEON multimeter. Furthermore, NO3 and NO2 where directly measured with Hach NO3 test strips and an E. coli sample was prepared (3M Petrifilm E.coli). Two unfiltered and four filtered (0.2 µm) samples were collected in 15 ml plastic sampling vials and transported in an icebox to the lab. For the unfiltered samples the alkalinity was determined with an alkalinity field titration kit (Hach, sulphuric acid cartridges (0.16 N & 1.6 N) and bromcresol green-methyl red indicator powder). Before storage at 4 C, the tubes for the ICP and DA analysis were acidified below pH=2 with concentrated nitric acid (HNO3, 69%), whereas the IC and backup sample tube where only sealed with parafilm. Back in the Netherlands the anion, cation, nutrient and heavy metal analyses were performed in the Water Lab of Delft University. The performed analyses are summarized in table 3.1.

3.2 Data validation

When all data was assembled, there was a check if the data was correctly measured. First of all some data were measured twice; the correlation between these outputs where plotted to see if the results harmonized. Secondly, ion mass balance calculation were performed to check whether the different analyses have been accurate. Lastly, the EC measurements have been checked by M. Wit, based on the measured ion concentrations.

3.3 Data analysis

To acquire insights into the difference of groundwater quality all over the island and processes responsible for this quality, multiple methods used in (ground)water qual-

ity analyses will be combined. First of all descriptive statistics are applied to determine correlation and statistical differences in the data. To further obtain insight into patterns and processes, graphical and Multivariate Statistical Techniques (MST) were applied. Where descriptive and graphical methods are restricted to a limited number of parameters, MST makes use of the complete data set. When these techniques are combined, they provide unique information about the water types and water chemistry on the island (Güler, Thyne, Mccray, & Turner, 2002).

3.3.1 Descriptive & graphical statistics

To get insight into the chemical properties, the central tendency and dispersion are calculated and the data is graphically displayed in box plots, scatter plots and correlation matrices. The descriptive statistics and box-plots give a first indication to see whether there is a difference within the measured parameters caused by geological formation and if there is a change over time, the latter being explained in section 3.4 . To test if this difference is significant, the non-parametric, pairwise Wilcoxon test is performed. The correlation between variables is analysed with the Pearson's method. Furthermore, the correlation of Ca, Na, Mg, SO4, K and HCO3 with Cl will be displayed in scatter plots. The Seawater Mixing Line (SML) will be displayed within these graphs. Deviations of the SML, passing through the origin to the seawater sample, reveals information about geochemical processes (Van Sambeek et al., 2000).

To acquire more insight into the SO4 sources, there will be looked ad the production and consumption of SO4. This is calculated with the following formula (Yu & Broers, 2018):

$$SO_{4cons.(-)orprod.(+)} = SO_{4m} - Cl_m * SO_{4sea}/Cl_{sea} \tag{3.1}$$

With the SO4 and Cl concentrations in mg/L, cons=consumed, prod=produced and m=measured.

Cl and Br have a conservative character when ionized in water and can thus give an indication about the source of the groundwater, as seen in appendix A.6 (Naily & Sudaryanto, 2018). That is the reason why the Cl/Br ratio was set out against the chloride concentration.

To assess whether the location of the well or well depth influence the EC values, the distance from the well to the coast and absolute well depth were calculated in ArcGIS Pro. These outcomes, together with the gathered data in the field, will be used as explanatory factors for groundwater quality in general and to support the dimensions found by the MST techniques.

To give insight into the possibility to use the water as drinking water, the concentrations of the samples are compared with the WHO drinking water standards, presented in appendix table A.2. The Sodium Absorption Ratio (SAR) is used as an indication for the suitability of water for irrigation, and calculated as follows:

$$SAR = Na/\sqrt{(Ca + Mg)/2} \tag{3.2}$$

With the concentrations of Na, Ca and Mg in meq/L. When the resulting SAR value is below 10, the water is "excellently" suitable for irrigation water, 10-18 it is "good" to apply as irrigation and above 18 it becomes "doubtful" either "unusable" to use it as irrigation water (Tasan, Demir, & Tasa, 2021).

The saturation index (SI) values are made available by M. Wit. The SI values of the samples with respect to multiple minerals were calculated with the PHREEQ program based on the groundwater data of 2021. The mineral for which the SI values were calculated are displayed in appendix table A.3. The values were used to explain spatial patterns in the data.

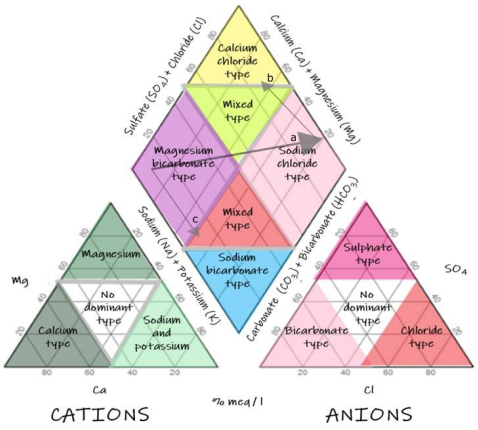

Figure 3.1: Piper plot showing the different water types based on the major ion concentrations. Conservative mixing with seawater is indicated by arrow a. Arrow b and c are an indication of cation exchange based on intrusion and freshening, respectively. Adjusted from: (Labs, 2018; Appelo & Postma, 2005).

3.3.2 Graphical Technique

Based on cations and anions, water types and processes can be distinguished by simple graphical displays. One of such techniques is the Piper diagram, using the relative percentage of the major cations (Ca, Mg Na+K) and anions (Cl, SO4 HCO3) in % meq/L. Based on this, each sample has its own location within the Piper diagram giving insight into the water types and process as seen in graph 3.1. When mixing with seawater would be conservative, groundwater samples would change from

Table 3.1: Performed lab analyses and methods

Machine	Component	Sample preparations			Method
		Filter	Accidification	Dilution	
ICP-MS	Ca, Mg, Na, K, Fe, Mn, Al, B, Ba, Be, Sr, Li, Mo, As, Cd, Co, Cr, Cu, Ni, Pb, Se, Sb, V, Zn, P & S	0.2 um	100 uL HNO3 (69%)	1% HNO3	-
IC	Cl, Br, F, NO3, NO2, SO4 & PO4	0.2 um	-	-	Methode van Swagatamn
DA	NH4 & PO4	0.2 um	100 uL HNO3 (69%)	MiliQ	1-20 mg P/L, 0-10 mg N/L
	Alkalinity	0.2 um	-	-	50-550 mg/L CaCO3

a Ca-HCO3 type to a Na-Cl type (arrow a). When samples deviate from this SWR line it is an indication that ion exchange is taking place. The result of cation exchange by seawater intrusion is seen in the Piper diagram by moving up, away from the SWR line (arrow b), because the water becomes enriched in Ca. Freshening results in the reverse cation-exchange process (arrow c), releasing Na to the groundwater. These two processes result in a Ca-Cl and Ca-HCO3 water type, respectively (Appelo & Postma, 2005).

3.3.3 Multivariate Statistical Techniques

MST analysis compare multiple variables within a data set. To acquire equal weight of each variable in the MST analysis, the variables need to be standardized. To account for this, the variables are first scaled to get a mean of zero and a standard deviation of one, before the MST is applied (Güler et al., 2002). The variables considered in the MST techniques are: pH, pE, T, EC, NO3, PO4, HCO3, Ecoli, F, Cl, SO4, NH4, Br, B, Ca, Fe, K, Mg, Na and Si.

Some samples had missing data, which is not allowed for MST analysis. To incorporate all samples in MST analysis the data was prepared: one missing HCO3 sample was replaced with the measured alkalinity value of the DA, NA values for E.coli were set to zero (4x) and missing pH (1x),pE (2x) and T (2x) vales were replaced by the mean value of the data.

Principal components analysis (PCA) is a MST method to get insights in a large set of correlated variables and to identify variables that explain most of the variance in a system (Ouyang, 2005). PCA summarizes the correlation within the data set into more interpretable axes of variation, while preserving the correlations in the original data. The axes are represented by the variables responsible for the correlation in the direction of the axis, called components. For interpretation of this analysis it is important that the components are distinct (Björklund, 2019). It is assumed that dimensions having a eigenvalue greater than 1 are significant (Tuddameri, Honnungar, & Hernandez, 2014; Tasan et al., 2021). Indicating that the dimension explains more than the component on its own (Amanah, Putranto, & Helmi, 2019) The PCA is applied to get insight in the groundwater processes and correlation between variables.

Another MST technique is clustering. Clustering is a method to group data based on the same characteristics. The samples within a group, a so called cluster, are similar in chemistry and they are distinctly different from the other groups (Güler et al., 2002). For K-means clustering the amount of clusters needs to be set to run the script, which influences the output(Zach, 2020). Hierarchical clustering results in a dendrogram, which can be investigated to decide upon the amount of representative cluster (STHDA, n.d.). To measure the goodness of the clusters the Dunn's method was used. The higher the Dunn's Index, the more distinct the clusters are (Pathak, 2018). To investigate what the clustering is based on, descriptive statistics of the groups where used.

3.4 Trend analyse

The hydrochemical data of the previous field surveys, performed by Abtmaier (1978) in 1977 and Louws et al. (1997) in 1992, is made available for this thesis by the SEALINK project. The data of the previous studies combined with the data of this field survey is used to analyse the trends in groundwater chemistry over the years using box plots, for EC, pH, Cl, HCO3, SO4, Mg, Ca, Na, K, Si, PO4, Br, NO3, NH4 and Fe. To test if there is a significant difference between the sampling years, the non-parametric, pairwise Wilcoxon test was performed.

To have a closer look at salt level changes over time the data sets have been coupled. The data of 1977 and 1992 could be linked based on the well code, 64 locations where measured twice. This was not possible for the 2021 sample survey, while only a few samples were re-sampled. Therefore, this data was coupled to the previous surveys based on distance. For all groundwater samples in 2021 the nearest well of the previous surveys and its distance to the well measured in 2021 was calculated with "Generate

near table" in ArcGIS Pro. This resulted in a put-code reference for each groundwater sample in 2021, making it possible to couple it to the previous surveys.

With the combined information of all these analyses the water chemistry and water types on the island can be indicated. Furthermore, it would be interesting to see whether there has been some significant changes over the years. The R script with all the analysis can be shared upon request.

Chapter 4

Results

In this chapter the results of the research will be presented in 4 sections. In the first section the results of the descriptive statistics, water types and spatial variation will be presented, including a paragraph over the exceedance of drinking water limits and the SAR. In section 2 the results which are used to get better insight into the groundwater process will be shown. These are the results of the chemical correlations, the saturation indexes, the scatter plots and chemical ratios. In section 3 the results of the PCA analyse will be shown and the clustering will be mentioned. In the last section the results of the trend analysis are presented.

4.1 Spatial variation

As mentioned before, in total 77 groundwater samples were collected of which the descriptive statistics are summarized in appendix table A.4. None of the variables is normally distributed and all variables are, except for Si, positively skewed, indicating that there are some extreme concentrations.

The groundwater pH ranges from 6.52 - 8.26, and the lowest pH values are measured in the Midden formation. The spatial variation in pH can be seen in figure 4.1a. It is seen that the pH is different in the west of Willemstad compared to the east. The latter can be divided in a difference between south-east and north-east of Willemstad. The pH of hand-dug wells appears to be higher compared to the pH in borehole wells, as seen in appendix figure A.4.

The range in EC values over the island is large (appendix figure A.4); the EC values are in general higher in the Knip and Midden formation compared to the other formations. The lowest EC of only 550 µS/cm is measured in Willemstad and the highest value (58529 µS/cm) in a well close to Santa Marta bay. The CLF is very diverse in EC values ranging from +- 500 µS/cm to +- 8700 µS/cm, the highest values can be found around Ronde Klip, in the north east of Willemstad. The spatial variation of EC values over the whole island can be found in figure 4.1b. There is no clear relation between the EC and well distance to the coast nor between the absolute well depth (MSL) and the EC. This figure is shown in the appendix figure A.5. The spatial variation in CL, K, SO4, Br, Mg, Ca and Na concentrations is analogue to the EC values.

At low EC values Mg, Ca, Na+K are equally abundant in the groundwater; when the EC increases the share of Na+K becomes dominant, while the ratio of Mg and Ca remain equal. For the anions HCO3 dominates at low EC values, whereas Cl dominates at high EC values. SO4 contributes less than 20% and only in some cases SO4 contributes more, which can be seen in the Piper diagram of figure 4.2a.

Figure 4.2a also shows that all water types are present on the island. The mixed Na-HCO3 type and Ca-HCO3 type are most abundant with 32.5% (n=25) and 31.1% (n=24) samples belonging in that group, respectively. Followed by 18.1% Na-Cl (n=14) and 15.6 % Ca-Cl (n=12). Three samples have Na-K-HCO3 as water type (3.9%) and GW041 has, as the only groundwater sample, a mixed Na-HCO3 water type. The spatial variation of water types over the island is seen in figure 4.2b.

The nutrient concentrations in the groundwater of Curaçao are also widely varying, see appendix table A.4. So is the range in NO3 concentrations large, 19.5 % of the samples (n=15) have a concentration below detection limit (0.03 mg/L) while 29.1% of the samples (n=23) have a concentration above 100 mg/L up to a maximum of 271.2 mg/L. The highest concentrations are found in the eastern part of Curacao around Willemstad, which can be seen in figure 4.1b. Furthermore, it can be seen that the concentration south-east of Willemstad is slightly lower than the NO3 concentrations north-east of Willemstad.

The range in NH4 concentrations (0.056 - 74.6 mg/L) is distorted by 4 samples having a concentration higher than 1 mg/L, which are sample GW004, GW032, GW043 and GW055B (appendix figure A.2).

PO4 concentration ranges from below detection limit

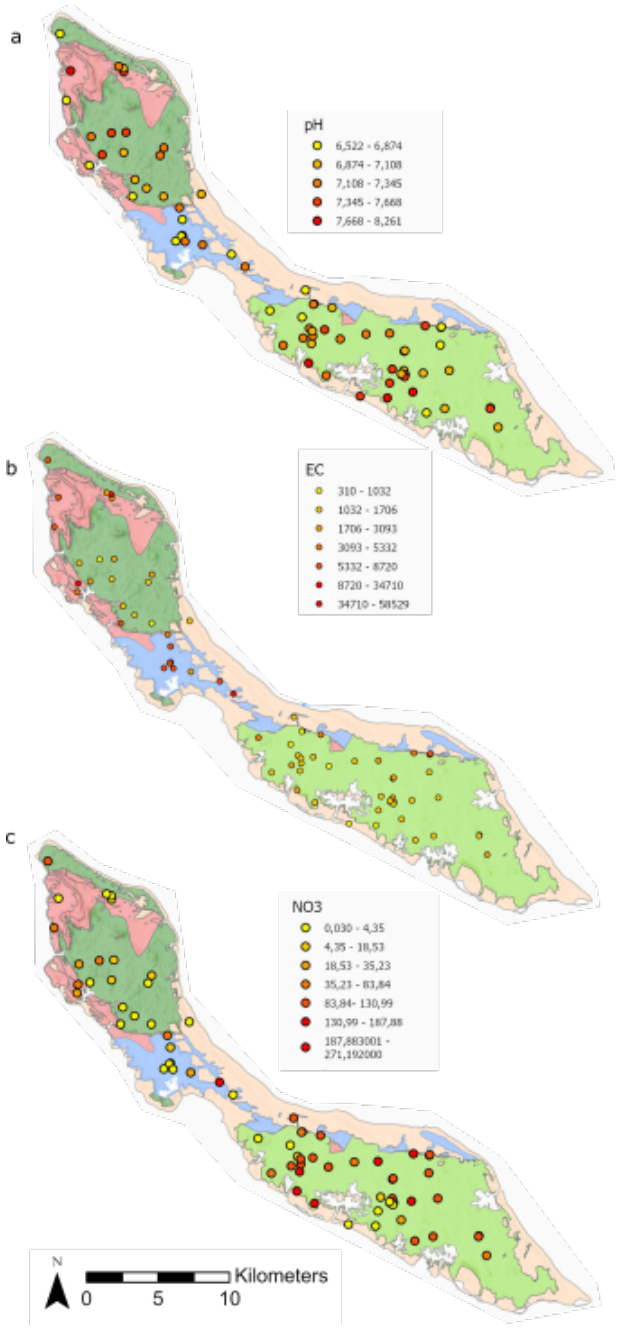

Figure 4.1: Maps of the spatial variation in a) the pH values b) the EC values and c) the NO3 concentrations for the groundwater samples of 2021

(0.001 mg/L) up to 28.41 mg/l. A concentration below detection limit is the case for 22.1% of the samples (n=17) and the PO4 concentration is higher than 1 mg/L for 14.3% (n=11) of the samples. The spatial variation in P04 shows a similar pattern with NH4.

The Fe concentration is higher in the Knip formation compared to the other formations. Besides, well GW045 in the Midden formation has an extremely high value for Fe, being 20.9 mg/L. The Si concentration is significantly lower in sedimentary formations compared to the CLF.

The maximum values of all measured variables exceed the limits allowed for drinking water (appendix figure A.2). There are only two wells who fulfil drink water standards, which are GW0042 and GW063. In the other samples the drinking water limits are exceeded by one or more variables. Mg and Cl limits are exceeded most often, in 81.0% (n=64) and 63.3% (n=50) of the wells, respectively. The NO3 limit is exceeded in 48% (n=37), which is predominantly on the eastern part of the island and 2 wells located in the west. Na is exceeded in 44.3% (n=35) of the samples, predominantly along the coast and in the Midden formation. Futhermore, E. coli is present in 70.1% of the samples (n=54). The SAR results indicate that almost all samples are "excellent" or "good" suitable for irrigation. Only 2 samples are "doubtful" to use and one well is "unsuitable". The plot with the SAR results is displayed in appendix figure A.7.

4.2 Hydro-chemical processes

The following methods are setup to be able to relate the concentrations of measured variables and the spatial variability with the chemical processes.

4.2.1 Ionic relations and ratios

In appendix table A.5 the correlation between the parameters is displayed. It is obvious that Cl (0.99), Na (0.99), Br (0.99), Mg (0.97), Ca (0.92), SO4 (0.86) and B (0.77) have a strong correlation with the EC. As such, these factors are also well correlated with each other. K has only a moderately strong correlation (0.45-0.68) with the beforementioned variables. Furthermore, K is also moderately correlated to PO4 (0.66) and HCO3 (0.57) and moderately correlated with pE (-0.54). Besides being moderately correlated with K, HCO3 and PO4 are strongly correlated with each other (0.83) and moderately correlated with the pE (-0.51 and -0.56, respectively).

To acquire more insight into the relation between Cl and the major cations and anions, the scatterplots are

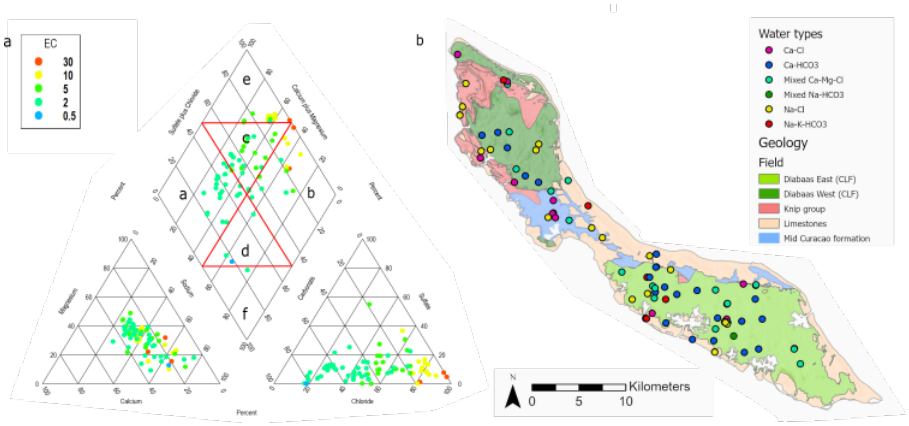

Figure 4.2: a) Piper diagram of the groundwater samples with the EC values a = Ca-HCO3, b =Na-Cl, c = mixed Ca-Mg-Cl, d = Na-K-HCO3, e= Ca-Cl and f = Mixed Na-HCO3 and b) spatial variation of water types over the island for all collected water samples

displayed in figure 4.5. It is immediately visible that the sedimentary formations (L, K and M) have higher Ca, Na, Mg, SO4, K and Cl concentrations. The HCO3 concentrations are within the same range for all formations, more or less between the 300 mg/L up to 700 mg/L.

In figure 4.5a and f, it can be seen that Ca and HCO3 concentrations are higher than the concentration expected by seawater mixing, this indicates that there are additional sources adding Ca and HCO3 to the groundwater.

The Na concentration is only higher than expected by seawater mixing for samples with a Cl concentration below +-300 mg/L (figure 4.5b). For the other Cl concentrations the Na concentration is lower than expected by seawater mixing.

For Mg and SO4 (figure 4.5c and d, respectively) there is a spread in concentrations around the SML. The spread around the SML for Mg is less for the Midden and Knip formation than for the CLF (DO and DW). For SO4 this spread in concentrations around the SML is larger for DO than it is for the DW. The K concentrations in all samples are below the SML, figure 4.5e. The spread in the CLF is bigger than the spread in the sedimentary formations. The concentrations in the sedimentary formations are closer to the line than the concentrations of the CLF.

As seen in appendix table A.5, Br is strongly positively correlated with Cl. To investigate the source of Br for each individual sample, the Cl/Br ratio is plotted against the Cl concentration, displayed in appendix figure A.6. Samples with the Br concentration under detection limit (0.003 mg/L) are left out of consideration (RW001, GW029 and GW051, figure A.2). As can be seen in appendix figure A.3, the Cl/Br ratio of "volcanic halites" (volcanic minerals) and "leaching of garbage and solid waste" is almost similar. The CL/Br ratio indicative for "coastal and arid climate" is in the same order of magnitude however the Cl concentration is lower and that of Br higher. The ratio of "urban wastewater" and "industrial halites" are even higher, with an higher Cl concentration. In this survey GW010, GW023, GW025, GW034 and GW025 score very high on the Cl/Br ratio, and there Cl concentration is low. These wells are mostly located in the northwest of Willemstad and two around the infiltration pounds. On the other hand, GWO50 and GW043 score below the 500 which is also an indication for pollution.

To obtain more insight in the behavior of Ca, Ca is plotted against the HCO3 concentration, as seen in figure 4.3. It is visible that the CLF samples are clearly following the 1:1 line, whereas the sedimentary formations are above this 1:1 line.

4.2.2 Saturation Indices

Most samples are oversaturated with regard to dolomite (CaMg(CO3)2), calcite (CaCO3), quartz (SiO2), goethite (a-FeO(OH)), and gibbsite (Al(OH)3). With respect to quartz, only the samples in the CLF are oversaturated, the samples in the other formations are in equilibrium with the mineral. Furthermore, multiple samples are oversaturated to phosphate minerals, 48.1% of the samples (n=37) is oversaturated with fluorapatite (Ca5(PO4)3F) and 35.1% of the samples (n=27) is oversaturated with respect to hydroxyapatite (Ca5(PO4)3(OH)).

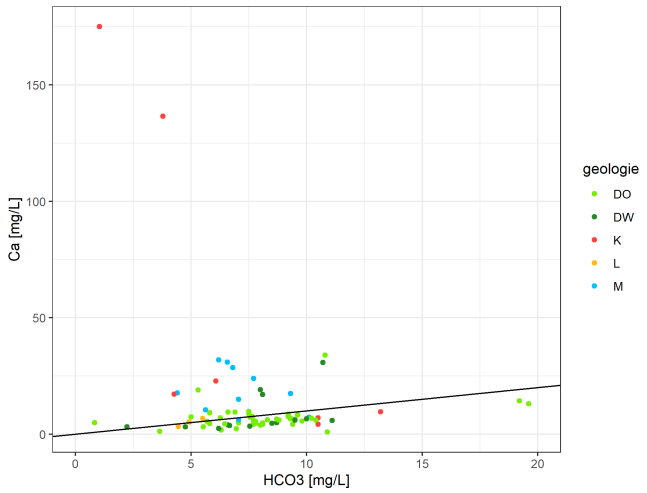

Figure 4.3: The Ca concentration plotted against the HCO3 concentration for the groundwater samples of the survey of 2021, the line is indicative for the 1:1 line.

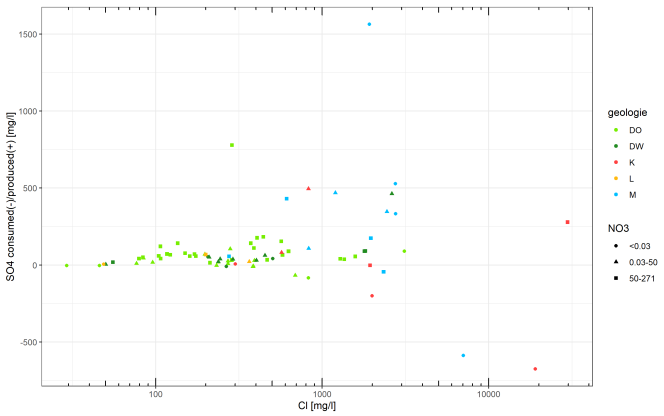

Figure 4.4: SO4 production or consumption plotted against the Cl concentration. The higher the Cl concentration the more SO4 the groundwater can contain and the more there can be consumed, when SO4 is produced it is an indication for an extra SO4 source beside seawater.

4.2.3 SO4 production or consumption

To obtain a better understanding of SO4, SO4 consumption and production is plotted against the Cl concentration, figure 4.4. It can be seen that in a lot of wells there is a production of SO4, meaning that there is an extra SO4 source besides seawater. In the wells of the midden formation the SO4 production is higher relative to the other formations. As can be seen, there is SO4 consumption in the wells where NO3 is already under detection limit (0.003 mg/L). However, there are some wells with an NO3 concentration below detection limit but there is still a high production of SO4. These samples are all collected around Willibrordus.

4.3 PCA and sample clusters

The PCA resulted in 5 significant dimensions with an eigenvalue greater than 1, which are displayed in table 4.1. The PCA plot is displayed in appendix figure A.8. In total 78% of the variation is explained by these axis. The first dimension, explaining 40.6%, is formed by the EC, the major anions and cations (except for HCO3) and a not that strong but negative contribution of Si. Dimension 2 (17.6%) is explained by HCO3, NH4, PO4 and Pe, the latter being negatively correlated. The third dimension is explained by Iron and NO3, the forth by pH and T and the fifth dimension by F. The hierarchical and K means clustering resulted in groups that were mostly based on the NO3 concentration and EC.

Table 4.1: PCA results, strong contribution to the dimension (-0.7<x>0.7) is presented in bold, moderate contribution is displayed in italics (-0.7<x<-0.5 and 0.5<x<0.7)

	Dim.1	Dim.2	Dim.3	Dim.4	Dim.5
pH	-0.127	0.155	0.163	**-0.742**	-0.041
NO3	-0.133	-0.312	*0.628*	0.312	-0.003
PO4	0.344	**0.864**	0.147	0.026	-0.066
HCO3	0.146	**0.894**	0.169	0.041	0.077
Ecoli	-0.028	0.270	-0.155	-0.045	-0.461
F	-0.065	-0.027	-0.225	-0.143	**0.841**
Cl	**0.962**	-0.195	0.106	-0.039	-0.041
SO4	**0.843**	-0.348	-0.046	0.004	0.038
NH4DA	0.332	**0.866**	0.165	0.098	0.000
Temp	-0.048	-0.096	0.174	**0.739**	0.092
EC	**0.981**	-0.136	0.101	-0.013	-0.013
pE	-0.444	*-0.597*	0.375	-0.227	-0.059
Br	**0.960**	-0.199	0.120	-0.037	-0.029
B	**0.829**	0.033	-0.117	-0.048	0.276
Ca	**0.908**	-0.187	-0.013	0.036	-0.030
Fe	0.242	-0.056	**-0.707**	0.287	-0.108
K	*0.656*	*0.558*	0.129	-0.004	0.134
Mg	**0.928**	-0.273	0.126	-0.052	-0.009
Na	**0.970**	-0.141	0.120	-0.046	-0.044
Si	*-0.550*	0.030	0.335	0.111	0.251
Eig.Val	8.1	3.5	1.5	1.4	1.1
Var. %	40.6	17.6	7.3	6.9	5.6
Cum. Var. %	40.6	58.2	65.4	72.4	78.0

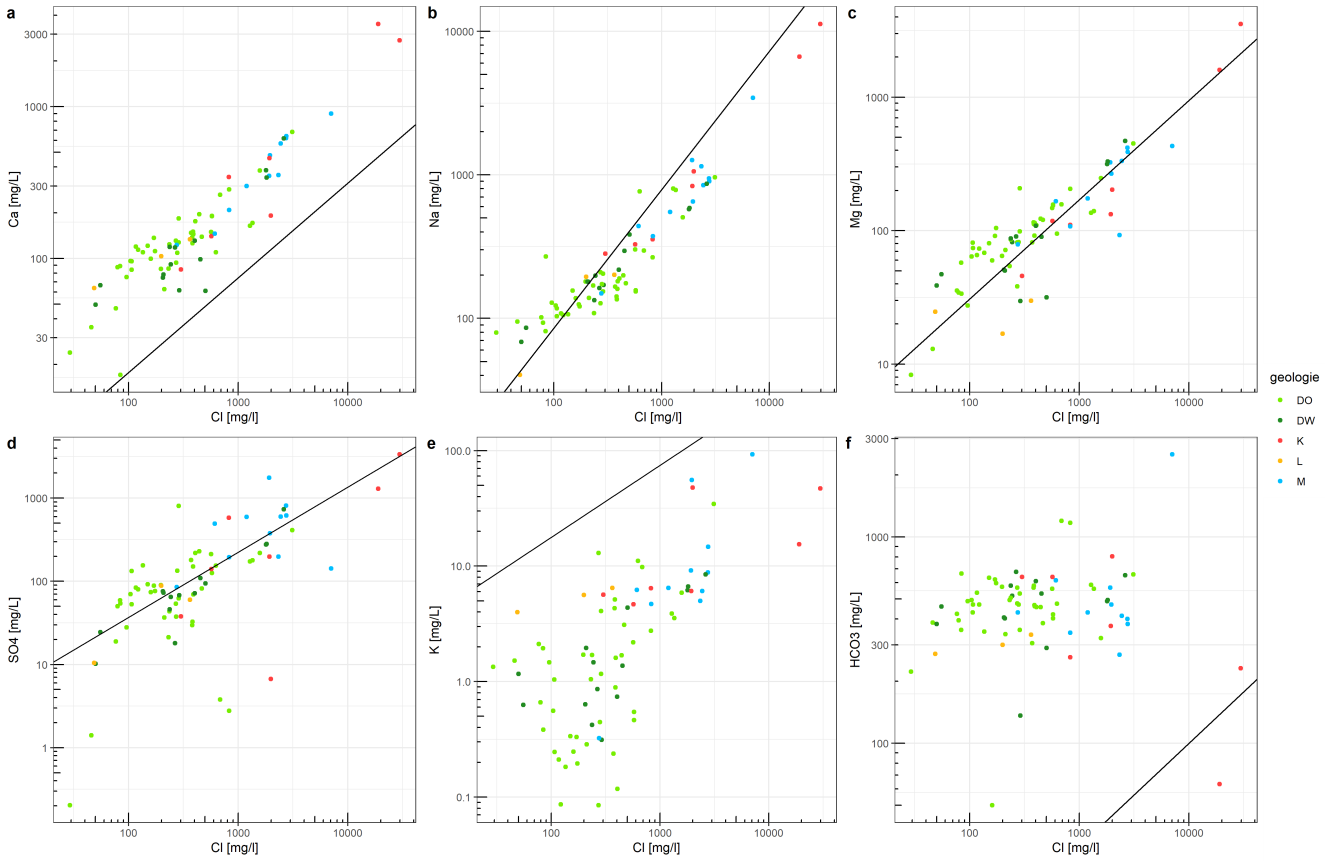

Figure 4.5: Correlations of Ca, Na, Mg, SO4, K and HCO3 with Cl for the groundwater samples of 2021, the line is indicative for conservative mixing with seawater (SML line)

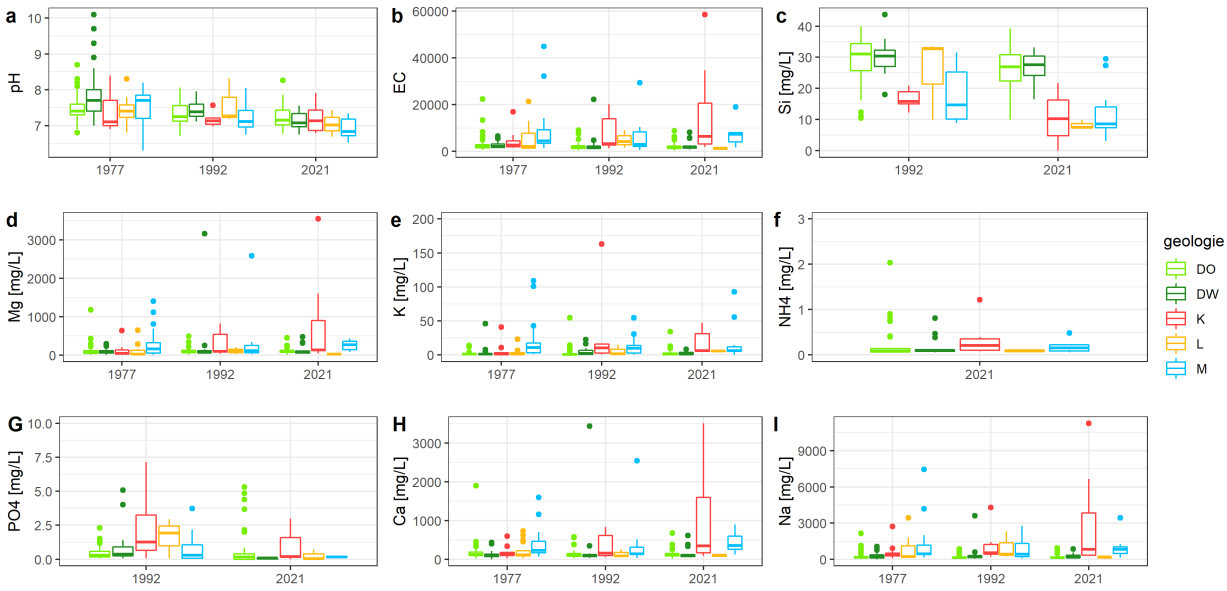

Figure 4.6: Boxplots of the pH, EC, Si, Mg, K, NH4, PO4, Ca and Na concentrations of the groundwater samples per geology per year, sample numbers per formation and year can be found in table A.1

4.4 Chemical trend

A significant difference compared to the previous surveys of Abtmeier (1977) and Louws et al. (1992) is found for pH, HCO3, K, Mg, NH4, PO4 and Si, as seen in appendix table A.4. Over the years, it is found that the pH, Si and PO4 concentrations are decreasing, whereas the HCO3, K, Mg and NH4 concentration are increasing. This can be seen in the boxplots of figure 4.6. There is not a significant change in EC values or Cl concentrations over the years (appendix table A.4). However, this only shows the general trend over the island and cannot indicate freshening and salinization that is possibly ongoing in certain parts of the island. That is why spatial variations of EC and Cl is considered over the years, which showed that the EC and Cl values increased in Willibrordus, the wells in Cristoffelpark and the wells around Ronde Klip.

Chapter 5

Discussion

In the first section the spatial variability will be discussed. In the second section the chemical results will be discussed more in-depth and the results of the different analyses will be coupled. In the third section the process found by the PCA and the clusters obtained by the clustering analysis will be analysed. In the last sections the trend over the years will be discussed.

5.1 Spatial variation

The spatial variation of EC values over the island (figure 4.2b) indicates that freshwater water (EC<1500 µS/cm, (Park, Lee, & Song, 2012)) can only be found in the CLF formation. However, within the CLF there are also still a lot of wells having brackish groundwater conditions ((EC<3000 µS/cm). The freshwater samples are classified as Ca-HCO3, Mixed Ca-Mg-Cl and some as Na-Cl types (figure 4.2). The Ca-HCO3 type is expected for fresh water, indicating the groundwater chemistry is influenced by the geology. Having fresh water with a Mixed Ca-Mg-Cl water type is thus an indication for salinisation taking place.

In the middle part of the island and along the west coast of the western part there is only saline groundwater (EC>3000 µS/cm). The water types of these saline groundwaters are dominantly Na-Cl and Ca-Cl as well as mixed Ca-Mg-Cl (figure 4.2), indicating that there are three different stages of seawater intrusion. The first stage is mixed Ca-Mg-Cl, which is groundwater in the transition phase between ambient groundwater and water effected by seawater intrusion, indicating that salinisation takes place. Groundwater with an Na-Cl water type is groundwater influenced by conservative mixing with seawater, indicating seawater intrusion. The third stage is the Ca-Cl water type, which is the result of groundwater affected by seawater intrusion with ongoing replacement of Na for Ca on the soil matrix by cation exchange.

The absence of a clear relation with the distance to the coast and with the absolute well depth, could be explained by the fact that the spatial variation in the stages of salinisation is high. Furthermore, it is visible that there is a freshwater lens present in the limestone formation in Willemstad (well GW063), whereas the Knip formation, also close to the coast, is saline.

There is only one sample with a mixed Na-HCO3 water type, which is an indication of freshening. This is a groundwater well in the south east of Willemstad, sample GW041 (figure 4.2b). This well is located close to a bay and because the groundwater chemistry is not influenced by seawater, there should be a freshwater source from land to cause this freshening.

Three possible options could explain this water type and they should be further investigated. First of all, it could be water infiltrating in the green area north of this well. Secondly, it could be an indication that the water from the infiltration pound is draining towards this well. The last option could be that it is a leaking cesspit.

To investigate the theories, multiple research steps are advised. First of all, more samples south-east of the infiltration pounds should be collected. This in order to obtain a better view on the area and the potential groundwater flow. When this is the only well with an Na-HCO3 type, high NO3 concentration and presence of E.coli it is likely that the groundwater is influenced by a leaking cesspit.

Secondly, calculations about the groundwater flow should indicate if the groundwater plume of the infiltration pounds could have reached this location. If this is not the case than it is more likely that the water is influenced by the green area above the well.

As a last research step, the groundwater age of the sample could be determined with isotopes, to see whether the age is coinciding with the groundwater plume.

The high values of NO3 in the eastern part of the island (figure 4.1c) are probably caused by the leachate of septic tanks and cesspits. On Curaçao there is only small scale agriculture (de Vries, 2000), thus the contribution of this factor as source for NO3 in this densely populated area is expected to be low. NH4 is nitrified to NO3 in aerobic conditions by the following chemical reaction: $NH_4^+ + {}_2O_2 \rightarrow NO_3^- + {}_2H^+ + H_2O$ (Robertson, 2021).

This nitrification also explains why the NH4 concentrations in groundwater are low even though its concentration is high in the effluent of the septic tank (Robertson, 2021).

The spatial variation in the concentration of PO4 is related to NH4 concentration, even though the PO4 concentration in septic tanks effluents is high (Robertson, 2021). This indicates that PO4 is removed from the soil solution just like NH4, 2 mechanisms are responsible for this.

The first mechanism is that PO4 will be adsorbed by the soil surface and organic matter (Robertson, 2021). The second mechanism is caused by the buffering of the acidic effluent by the dissolution of minerals. The lowered pH, and the released ions by the buffering, increase the precipitation rate of PO4minerals (Robertson, 2021). This also explains the correlation of PO4 with pH (table A.5). The lower pH also increases the positive charge of the soil matrix and thus increases the available binding sites for PO4.

The PO4 values are above 1 mg/L for two wells close to the water infiltration ponds, the golf course and the waste dump. This shows that the infiltrating treated waste water and water coming from the landfill is containing a lot of PO4, which saturates the available binding sites of the soil matrix and causes PO4 to leach into the groundwater. To indicate the length of the PO4 contamination plume in the subsurface more samples need to be collected.

As can be seen in boxplot c of figure 4.6 the Si concentration in the CLF formation is significantly higher than in the other formations. This is caused by the interaction of groundwater with the surrounding geology and the fact that the CLF is SiO2 rich. Besides, weathering of basalt is easier compared to quartz, which is the Si constituent of the other formations (Appelo & Postma, 2005).

To acquire more insight into the groundwater flow over the island a higher sampling density is acquired. The reason for this is that the spatial variation in the concentrations of the variable is large. For example, right now it is not yet possible to determine where the water of the spring samples is coming from.

The timing of sampling is important if there is a possibility of surface runoff flowing into the well. It is assumed that the well in which GW001 and GW029 are collected (appendix figure A.2), is highly influenced by rainwater. The reasons for this assumption are that the EC is quite different between the samples (593 µS/cm and 310 µS/cm, respectively), the Br concentration of GW029 is below detection limit (0.003 mg/L) and videos showed that the well is acting as a drain for surface runoff of the garden. Therefore, this should be kept in mind during fieldwork when investigating the well. Furthermore, for the spring samples it would also be interesting to see if the concentrations of the variables change over time.

5.2 Hydro-chemical processes

Salinisation is an important process over the island, as can be concluded from the strong correlations between Cl, Na, Br, Mg, Ca, SO4, B and K (table A.5) and the scattering of the groundwater samples around the SML for Na, Mg, SO4 and K (figure 4.5). These correlations are easily explained by the fact that the groundwater is influenced by seawater intrusion, sea spray and rainwater which has a composition resembling diluted seawater.

The scattering around the SML (figure 4.5) indicates that there are some chemical processes ongoing besides seawater intrusion. It is seen that Mg is on the SWR line while the Ca is above the line and K and Na are under the line (figure 4.5c,b and e, respectively). This shows that Mg concentration is based on salinisation, caused by seawater intrusion, sea spray and rain. In first instance Ca, Na and K are also influenced by these processes, however, the Na and K concentrations are lowered and the Ca is increased by the cation exchange process. In this process bound Ca to the soil matrix is substituted by Na and K, releasing Ca to the groundwater and lowering the Na and K concentration.

The Na concentration is higher than expected based on the SML for samples with Cl concentration smaller than 300 mg/L, as also found by (Van Sambeek et al., 2000). This is caused by freshening of the aquifer compared to the ambient groundwater. The Ca and HCO3 concentrations are all higher than the concentration expected by the SML (figure 4.5a and f), this is caused by the fact that there are many processes influencing the Ca and HCO3 concentration in the groundwater system. First of all, as explained above, cation exchange influences the Ca concentration. Furthermore, also the dissolution and precipitation of carbonate minerals influences the concentration of Ca and HCO3.

While the dissolution of minerals effects the concentration of HCO3 and thus the pH, it is interesting that there is no correlation with the pH (Kura, Ramli, Ibrahim, Aris, & Mustapha, 2013; Sarker et al., 2022). However, there is no negative relation between Ca and Na either (appendix table A.5). That means that the effect of salinisation makes it hard to distinguish those two chemical processes based on the correlation alone.

The plot of Ca against HCO3 (figure 4.3) shows that the CLF is nicely aligned with the 1:1 line, whereas the Ca concentration is above this line for the sedimentary

formations. This indicates that dissolution of minerals is the main mechanism for Ca in the CLF, while cation exchange is the main mechanism for additional Ca for the sedimentary formations. The saturation indices indicate that the groundwater is oversaturated with respect to gypsum, calcite and dolomite. Dissolution of those minerals could thus contribute to the elevated Ca and HCO3 concentrations with respect to the SML.

Sambeek at al. (2000) found that the high iron concentration coincides with very negative redox potentials in the Knip formation. The average highest Fe concentration are again found in the Knip formation, however, this time the Fe concentrations do not correlate with the negative redox potentials. The most obvious reason for this deviating pE trend, is because pE is difficult to measure in the field. There are 5 wells with negative pE having a high Fe concentration (2X DW, 2XM and 1X K), however, there are also 3 wells having an even more negative pE and barely any Fe. These wells are located around Willibrordus and two along the road to Soto (GW051 and GW052), which area is interesting to further investigates also based on the high SO4 concentration as explained below.

The SO4 concentration is highest in the Midden formation (figure 4.6), which can be explained by salinisation. However, the high SO4 production around Willibrordus (figure 4.4) is indicative for an extra SO4 source beside seawater intrusion. All groundwater samples are undersaturated of gypsum, however, the undersaturation of the Midden formation is less negative to gypsum compared to the other formations. The samples of the Midden and Knip formation are in equilibrium with barite, while the CLF samples are all undersaturated for barite. The reason for the spatial variation in SO4 and the high concentrations around Willibrordus should thus be further investigated.

Based on the Cl/Br ratio (figure A.6) it is again seen that the samples with higher EC, indeed fall in the expected range of seawater intrusion. As for the other samples, it can be seen that most samples are a mix of Cl/Br ratios indicative for "coastal and arid climate", "volcanic haliees" and "leaching of waste" (appendix figure A.3). This is in accordance with the situation on Curaçao, however, it is hard to distinguish between these processes while they happen at the same time. The Cl/Br ratio does not give a clear distinction between these processes, this is up for further investigation. However, the Cl/Br ratio could be used for extremes, it is seen that 2 samples fall below the 500, which are sample GW043 and GW050 (appendix figure A.2). Indicating that well GW043, having the lowest CL/Br ratio, is clearly influenced by the waste dump and Br leaching from it.

5.3 PCA and sample clusters

There are 5 significant PCA dimensions as can be seen by their eigenvalue (>1) in table 4.1. In total 78% of the variation is explained by these axises. DO is not taken into account by the PCA analysis. It decreased the percentage explained by the axis, because it gives a random noise to the data. This is caused by two reasons that have to do with the sampling method. First of all, for most samples the DO is measured in +-one litre standing water, while other samples are measured during continues pumping of water, the latter resulting in lower DO values. The second reason is that DO is hard to measure in the field because the time it takes before the reading stabilizes is long. However, when it would be incorporated it would oppose NH4 and PO4 as expected (appendix figure A.8). NO2 is left out of the PCA analysis because the time passed before measuring is too long for this nutrient and most values are below detection limit (0.010 mg/L).

The first dimension is explained by EC, Cl, SO4, Br, B, Mg, Na, Si, K and Ca (table 4.1), indicating that multiple process are incorporated in this dimension of which salinisation is most dominant. The incorporation of Ca and Na could indicate salinisation and cation exchange, the last one being active in the sedimentary formations as seen before. However, the arrows are pointing in the same direction, indication that this processes is overruled by salinisation. The pH and HCO3 is not incorporated within this axis, which would be the case if weathering would be represented by this dimension(Kura et al., 2013; Sarker et al., 2022). However, it was already seen in the correlation (appendix table A.5) that this relation was not strongly present. Striking is that Si is incorporated in this axis, indicating that with this axis the PCA emphasizes the difference between the geological formations. While in the lava formation the seawater intrusion is less and the silicate concentration is significantly higher compared to the sedimentary formations. Br is strongly represented in this dimension, pointing in the same direction as EC (appendix figure A.8), indicating that seawater intrusion is the dominant source of Br in the groundwater on the island.

In dimension 2, the presence of PO4, NH4, HCO3 indicate that this term is associated with pollution by septic tanks. In human effluence PO4and NH4 levels are high, where NH4 is the main N-constituent of the effluent. As explained in section 5.2, the effluent of septic tanks is acid, resulting in buffer mechanisms to act in the subsoil(Robertson, 2021). This explains why HCO3 points in the same direction as PO4and NH4. Under aerobic conditions, NH4 is converted to NO3, this is the

reason that NO3 concentration is pointing in the opposite direction of NH4 and PO4 (appendix figure A.8).

Dimension 3 is explained by Iron and NO3. From the correlation matrix it was shown that the NO3 and Fe were non-significant but slightly negatively correlated. This dimension could be explained by the process described by Sambeek at al. (2000). They found high Fe concentration in the Knip and Midden formation, coherent with negative pE values and high pH values. The reduced environment could be explained by the presence and breakdown of organic carbon. Also this year the higher Fe concentrations are found in the Knip and Midden formations, indicated by the direction of the arrow. As mentioned by Sambeek at al. (2000), the presence of elevated NO3 concentrations is probably caused by the recent mixing with polluted water. This indicates the slightly negative correlation of Fe and NO3, while the enrichment with fresh groundwater inhibits the mobilization of Fe.

Dimension 4 exist out of the pH and temperature. The pH is different in the different quarters of Willemstad (figure 4.1), which is interesting to further investigate in the context of watersheds and possible SGD fluxes. Furthermore, the pH is different for the different well types; borehole wells have a slightly higher pH compared to hand-dug wells, it is important to further investigate the reasons behind this difference, because than a correction can be made to acquire the real groundwater pH, uninfluenced by the well type and the retention within that well.

The saturation indices showed that multiple samples are oversaturated with respect to fluorapatite and hydroxyapatite, the dissolution of these phosphorus mineral could possibly explain the 5th dimension. However, there should be investigated which samples have a high contribution to this axis and if these samples are the samples saturated to fluorapatite.

Overall, the distinction between the geological formations, based on salinisation stage, comes clearly forward in the PCA (appendix figure A.8). When the NO3 concentration, instead of the geology, would be plotted in the PCA analyse figure, it would come forward with a clear pattern. That is why it is unexpected that it does not come forward as a most important contributor to one of the dimensions.

For the clustering analyses, the NO3 was the most important variable where the clustering was based on, resulting in two large group mainly diving east and west curacao. Also a couple of samples were put in the same group based on there extreme EC values. However, to test if it the clustering results can indicate catchments, there should be investigated where the smaller subdivisions are based on and if this division makes sense spatially. Furthermore, it would be interesting to see what the cluster results will be when the heavy metals are added to the analysis. If this does not result in any information about catchment and possible water-flow paths, this method will not be a valuable addition in the groundwater research on Curaçao.

It is advised to further investigate the possibilities of PCA and cluster analysis on the island of Curaçao. It would be interesting to see what the dimension and cluster results are when the PCA would be separately performed for the geological formations and if it then would be able to distinguish different catchments when the heavy metal concentrations are added.

5.4 Chemical Trend

This sampling period was wetter compared to normal, while there was a weak La Niña (WMO, 2021)). The precipitation amount in 2021 had a total sum of 623.2 mm, which is 3,5 % more compared to average. This is contrary to the previous surveys, which were drier compared to the average rainfall sum.

In the sedimentary formations the salinisation process continued compared to 1977 and 1992. The decrease in the Si concentration and the increase in EC, Cl, Ca, Mg and K concentration for the sedimentary formations (figure 4.6) are indicative for seawater intrusion, while the concentration of Si in seawater is below detection limit and the concentrations of Ca, Na, Mg, and K are high in seawater. Clearly visible in the EC and Cl concentrations compared to previous studies is that around Willibrordus, Ronde Klip and Christoffel park it is seen that the salinisation process increased.

To investigate freshening and less distinct salinisation, more in-depth analysis of the results is needed. The correlation of EC values for wells between the years was hard to establish, while multiple wells did get assigned to the same well from past surveys. This resulted in results that where difficult to interpret. Furthermore, there should be made clear what percentage of change is seen as either freshening or salinisation and what is disregarded as change because of difference in measuring device and most important the difference in measuring location and the noise caused by that. It is also adviced to zoom in on areas instead of looking at data of the whole island.

For NH4, the measured concentration differences of 1992 compared to 2021 are influenced by the measurement method for NH4. In the data set of 1992, a lot of values are under detection limit (0.25 mg/L) and the gradient is not really continuous. The NH4 measurement steps in mg/L where: 0.25, 0.5, 1, 1.5, 3, 5, 10, 30, 60, 400. This makes the comparison between the years impossible for the formations beside the Knip formation.

Over the years the pH is decreasing and HCO3 concentrations are increasing (figure 4.6). This is the ef-

fect of continuous leaching of septic tanks and irrigation. This continuous flow of fresh water brings along NH4 and organic matter that will start to oxidize and mineralize. Buffering mechanisms will result in an increase of the HCO3 concentration. nevertheless, this long term leaching of acids results in acidification and decreased the pH of the groundwater.

In the previous studies the SAR indicated that a larger percentage of samples were not suitable for irrigation, while now all samples except for 3 are suitable for irrigation. This means that the trend found by Louws et al. (1997) continued, however, the ranges they applied are not indicated in their work. However, when there is assumed that the same classification is used, it indicates that the ratio of Na and Ca+Mg changes. Probably caused by cation exchange, improving the groundwater for its suitability for irrigation. However, when this is the process accounting for it, this also means that more Na is bound to the soil, which will degrade the stability of the soil.

Chapter 6

Conclusion

The main goal was to find the reasons behind the hydrogeochemical status of Curaçao. In this study, the concentrations of hydrochemical variables of groundwater samples collected in 1977 (Abtmaier, 1978), 1992 (Louws et al., 1997) and 2021 were used as input. In total 22 physical, chemical and biological variables of the samples from 2021 have been analysed and their relations have been examined to acquire insight into the chemical processes influencing the groundwater quality. The comparison with the previous surveys has been performed to see if there are ongoing long term processes influencing the groundwater quality.

The influence of the interaction with the geology is clearly seen in the CLF, where the concentration of Si in the groundwater is significantly higher than in the sedimentary formations. This is caused by the weathering of the basalt. The groundwater in the CLF is also influenced by the dissolution of carbonate minerals, controlling the Ca concentration of the groundwater. Contrary, in the sedimentary formations it is cation-exchange which is controlling the Ca concentration. Salinisation is highly effecting the groundwater in sedimentary formations and to some extend in the CLF. In the limestone formation in the south of Willemstad there is a freshwater lens present.

Most groundwater samples are oversaturated with respect to dolomite, gypsium, calcite, magnesite, dolomite, quartz, fluorapatite and hydroxyapatite. That is why it is important to investigate the mineral solubility in more detail, to be able to explain the concentration variations over the island more accurately.

The anthropogenic effect is most clearly seen in the pH, NO2 and PO4 concentrations. The leaching of cesspits and septic tank effluent, recharges the groundwater with high concentrations of NH4 and PO4. NH4 becomes quickly nitrified to NO2 under aerobic conditions, whereas PO4 either binds to the soil surface or precipitates. The PO4 concentration of the groundwater is thus depending on the pH, availability of binding sites and the load of contaminated water. Areas which had high PO4 concentrations are most likely subjected to a high PO4 load, causing the binding sites to be already fully saturated.

In this survey it came apparent that the different quarters of Willemstad have different ion compositions and pH. Furthermore, it is highly likely that the infiltration ponds influence the groundwater quality in the surrounding area. This should be further investigated to acquire insights into the catchments and groundwater flow.

The PCA results indicate the aforementioned processes clearly, however, for further research it is advised to perform this analysis for the separate formations. This reduces the effect of testing the salinisation differences between the formations and makes it perhaps possible, with the addition of heavy metals, to investigate different water flow paths.

Over the years, seawater intrusion has become more prominent in the Knip and Midden formation. To make a statement about freshening, the research between the correlation over the years needs to be extended. The ongoing leaching of cesspits and septic tanks, is decreasing the pH of the groundwater over time.

The hydrochemical status of Curaçao is thus explained by recharge, salinisation, geological interactions, chemical processes and pollution. With these insight it is advised to further investigate the explanatory factors for the high diversity in the groundwater compositions on a smaller spatial scale. This in order to highlight areas that have been changed drastically in groundwater composition over the years and areas that are of interest for submarine groundwater discharge.

Acknowledgment

First of all, I like to thank my supervisors Victor Bense and Martine van der Ploeg and PHD candidate Titus Kruijsen for giving me the opportunity to join the SEALINK project and the forthcoming activities. I also would like to recognize their help and feedback during my MSc thesis. Furthermore, I would like to tank Titus Kruijsen, Mike Wit and Anne-Fleur van Leeuwen for the amazing fieldwork time, without them it would have been impossible. I especially want to thank Mike Wit and Boris van Breukelen for helping me out with analysing the data and the TU Delft lab technicians for explaining me the lab procedures. I especially want to thank Roel Dijksma, who supported me through an emotionally, difficult period making it able to continue my thesis. Furthermore, I want to thank my fellow students who gave useful feedback during the thesis Ring. Lastly, I want to thank all well owners for their hospitality and making it possible to perform this research.

Appendix A

Appendix

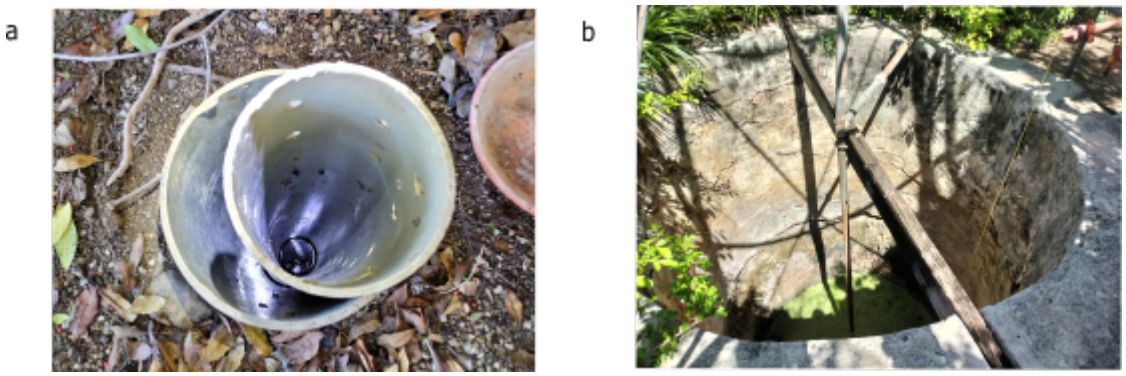

Figure A.1: An example of a borehole (a) and a hund-dug well (b) as can be found on Curaçao.

Table A.1: Total and percentage amount of groundwater samples collected per geological formation by Abtmaier(1978), Louws et al. (1997) and in 2021. The Curaçao Lava formation, covering 54% of the island, entails the Diabaas East (DO) and Diabaas West (DW). The sedimentary formations are the Knip formation (k), Limestone formation (L) and Midden formation (M), which cover 10.6, 27.4, 8.1 % of the island, respectively.

Year	Geology					
	Total	DO	DW	K	L	M
1977	233	134 (57.5%)	49 (21.0%)	13 (5.6%)	18 (7.7%)	19 (8.2%)
1992	97	50 (51.5%)	21 (21.6%)	6 (6.2%)	3 (3.1%)	17 (17.5%)
2021	79	44 (55.7%)	14 (17.7%)	7 (8.9%)	3 (3.8%)	11 (13.9%)

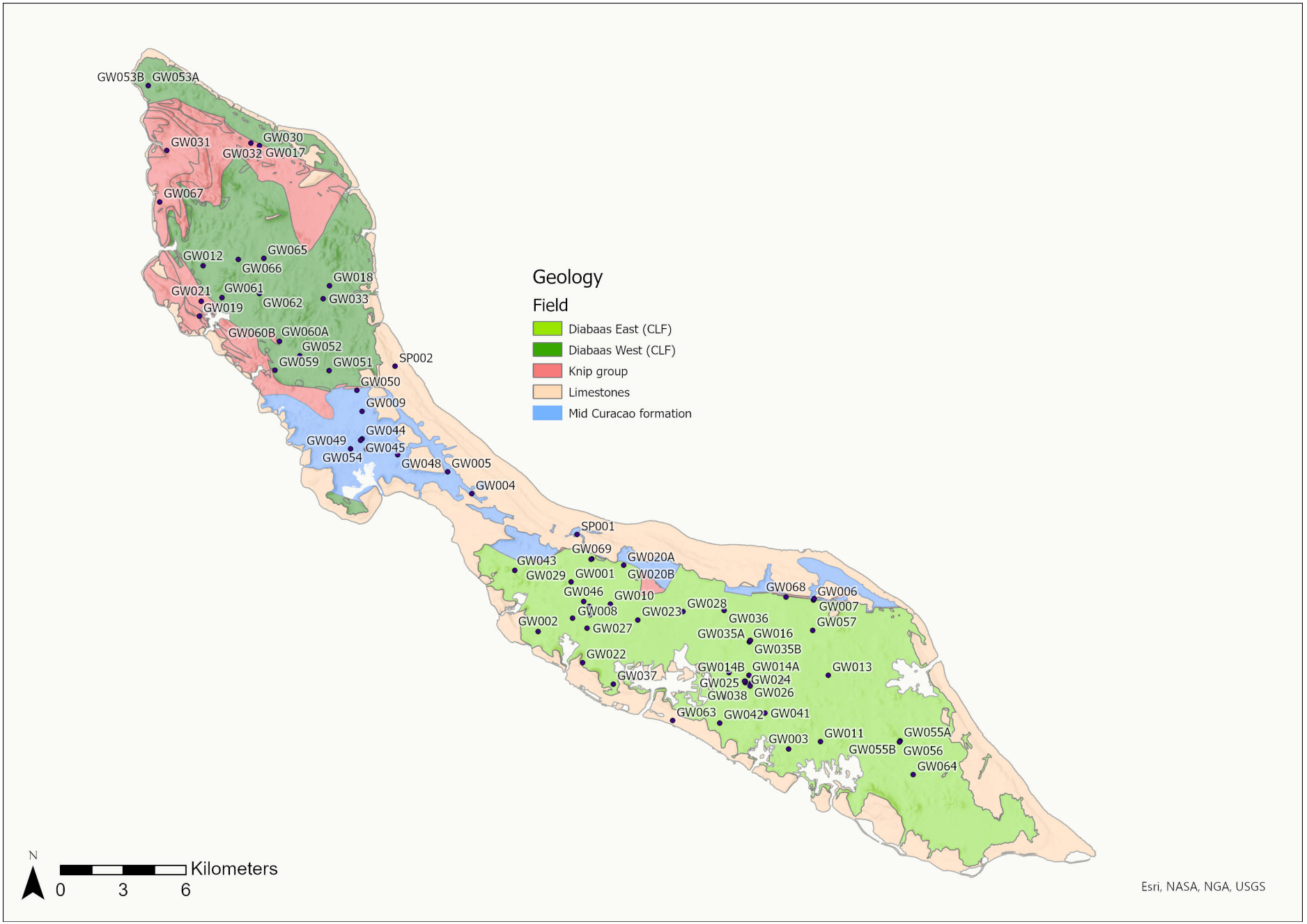

Figure A.2: Groundwater sample locations of 2021 with their sample code, geology based on geology map of Beets (1977).

Table A.2: Maximal allowable drink water concentrations as set by the WHO in mg/L.

	Max. admissible concentration
Mg	50
Na	200
Cl	250
SO4	250
NO3	50
NO2	0.5
Fe	1.5
Mn	0.05
Fe	0.2

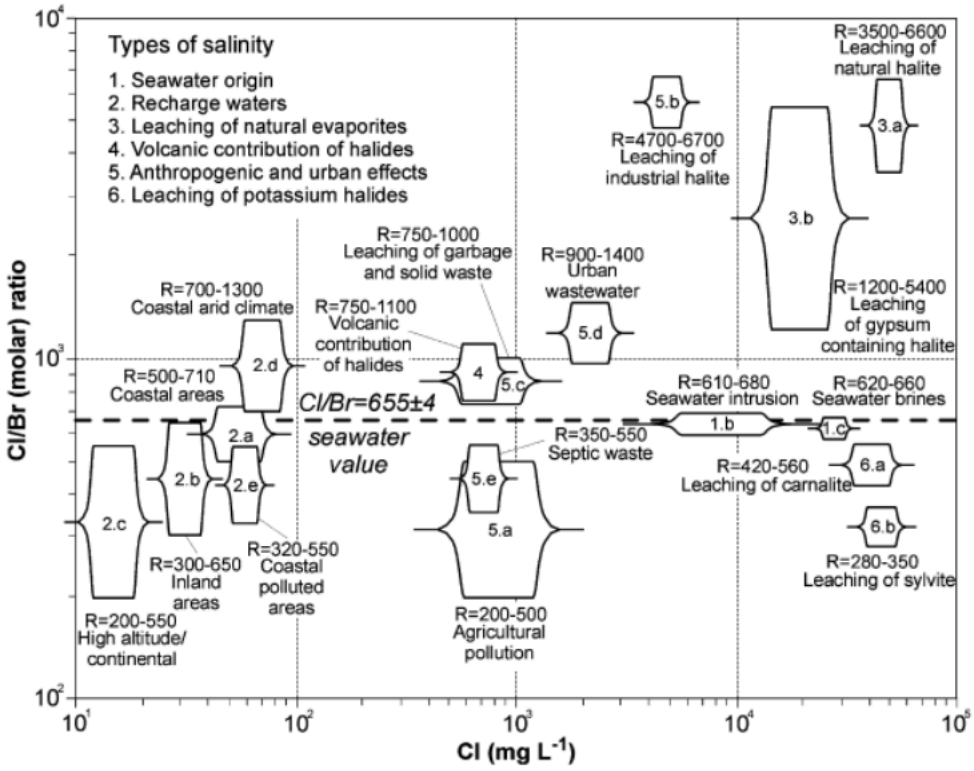

Figure A.3: Cl/Br ratio and their implications.

Table A.3: Minerals taken into account in the PHREEQ model run.

Type:	Mineral:
Carbonaten	Calcite, aragonite, dolomite, Magnesite, siderite and rhodochrosite
Sulfaten	Gypsum, anhydrite and barite
Fosfaten	Fluorapatite and hydroxyapatite
Silicaten	Quarts and amorf SiO2
Hydroxides	Fe-,Mn-, Al-hydroxides
Additional	Fluorite en halite

Figure A.4: Boxplot of the pH range for the borehole and hand-dug wel.

Table A.4: Descriptive statistics of variables of all groundwater samples collected in 2021. Significance ($p<0.05$) is indicated with * if data is significant different compared to 1977 ** if data is significant different with 1992 and *** is significantly different compared to the data collected in 1977 and 1992.

Variable	Unit	#n	Mean	Median	St.Dev	Min - Max	Sign.
pH	-	78	7.16	7.14	0.33	6.52 - 8.26	***
HCO3	mg/L	77	502.77	469.85	292.92	50.04 - 2514.02	*
EC	µS/cm	79	4080.91	1706.00	7710.70	310.1 - 58529	
Cl	mg/L	79	1352.88	372.62	3974.54	29.25 - 29740.44	
F	mg/L	79	0.26	0.11	0.37	0.001 - 1.60	
Br	mg/L	79	4.82	1.06	14.14	0.003 - 107.60	
SO4	mg/L	79	235.53	88.50	458.65	0.203 - 3356.52	
PO4	mg/L	79	1.04	0.14	3.59	0.001 - 28.41	**
NO3	mg/L	79	55.95	29.87	60.35	0.03 - 271.19	
NO2	mg/L	79	0.025	0.01	0.14	0.01 - 1.21	
NH4	mg/L	77	1.23	0.1	8.49	0.06 - 74.57	**
B	mg/L	79	0.70	0.52	0.56	0.05 - 3.378	
Ca	mg/L	79	265.81	130.79	497.77	17.10 - 3509.01	
Fe	mg/L	79	0.54	0.04	2.48	0.004 - 20.89	**
K	mg/L	79	6.61	1.94	14.17	0.08 - 92.67	*
Mg	mg/L	79	189.19	91.88	430.32	8.32 - 3544.08	*
Na	mg/L	79	580.57	180.73	1479.65	40.42 - 11264.13	
Si	mg/L	79	22.27	24.82	9.36	0 - 39.24	**
T	°C	77	30.20	30.00	2.01	27.06 - 43.9	

Table A.5: Correlation diagram, high to very high correlation are marked in bold (x<-0.7 and x>0.7).

	pH	NO3	PO4	HCO3	Ecoli	F	Cl	SO4	NO2	Temp	EC	pE	Br	B	Ca	Fe	K	Mg	Na	Si
pH	1																			
NO3	-0.1	1																		
PO4	0.07	-0.22	1																	
HCO3	0.1	-0.2	**0.83**	1																
Ecoli	0.05	-0.18	0.22	0.15	1															
F	0.04	-0.09	-0.1	-0.04	-0.05	1														
Cl	-0.09	-0.04	0.19	-0.02	-0.05	-0.09	1													
SO4	-0.18	-0.01	-0.01	-0.15	-0.1	-0.01	**0.84**	1												
NO2	0	0.05	-0.03	-0.04	-0.03	-0.05	-0.04	-0.05	1											
Temp	-0.27	0.21	-0.07	-0.06	0.02	0	-0.02	-0.01	-0.13	1										
EC	-0.12	-0.04	0.24	0.05	-0.05	-0.08	**0.99**	**0.86**	-0.05	-0.03	1									
pE	0.12	0.34	-0.56	-0.51	-0.1	0	-0.27	-0.17	0.12	0.01	-0.31	1								
Br	-0.1	-0.03	0.18	-0.02	-0.05	-0.09	**1**	**0.84**	-0.04	-0.02	**0.99**	-0.26	1							
B	-0.13	-0.22	0.24	0.14	-0.08	0.14	**0.73**	**0.72**	-0.09	-0.06	**0.77**	-0.41	**0.73**	1						
Ca	-0.17	-0.07	0.15	-0.04	-0.07	-0.07	**0.93**	**0.75**	-0.04	-0.02	**0.92**	-0.33	**0.92**	0.68	1					
Fe	-0.18	-0.19	-0.04	-0.07	-0.01	-0.01	0.17	0.24	-0.02	0.02	0.18	-0.37	0.16	0.17	0.26	1				
K	0.02	-0.14	0.66	0.57	0.05	0	0.5	0.35	-0.05	-0.06	0.56	-0.54	0.51	0.62	0.45	0.04	1			
Mg	-0.09	-0.01	0.11	-0.06	-0.07	-0.07	**0.98**	**0.89**	-0.04	-0.02	**0.97**	-0.19	**0.98**	**0.71**	**0.87**	0.16	0.45	1		
Na	-0.07	-0.05	0.24	0.03	-0.04	-0.1	**0.99**	**0.84**	-0.04	-0.02	**0.99**	-0.29	**0.99**	**0.75**	**0.91**	0.15	0.54	**0.97**	1	
Si	0.05	0.17	-0.16	0.1	-0.05	0.09	-0.46	-0.5	0.07	0.14	-0.48	0.26	-0.45	-0.45	-0.45	-0.26	-0.33	-0.39	-0.48	1

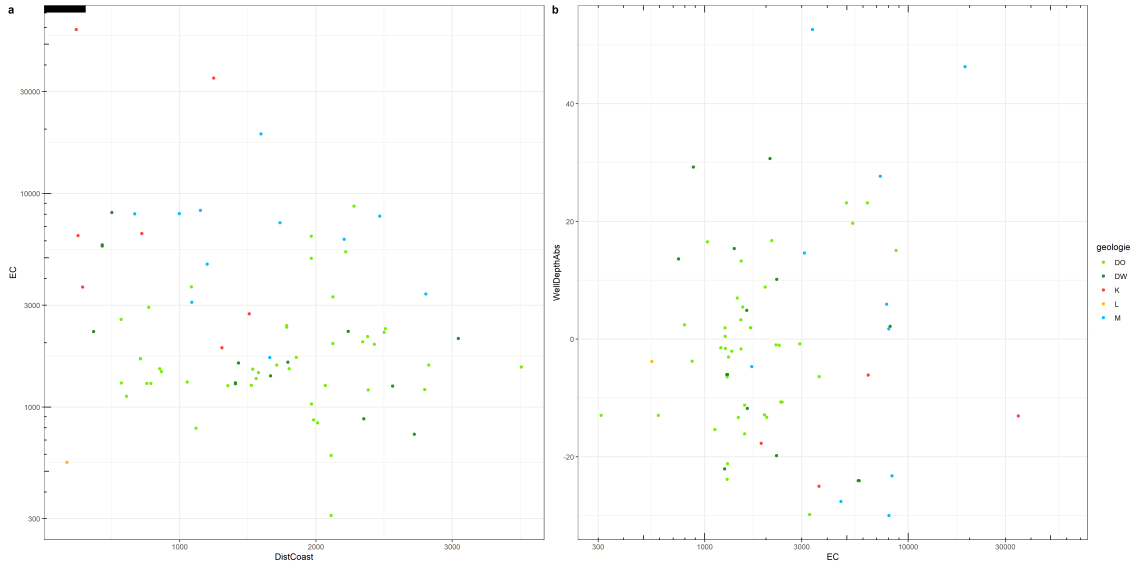

Figure A.5: EC concentration plotted against the distance to the coast (correlation = -0.12), and the absolute well depth plotted against the EC (correlation = 0.08).

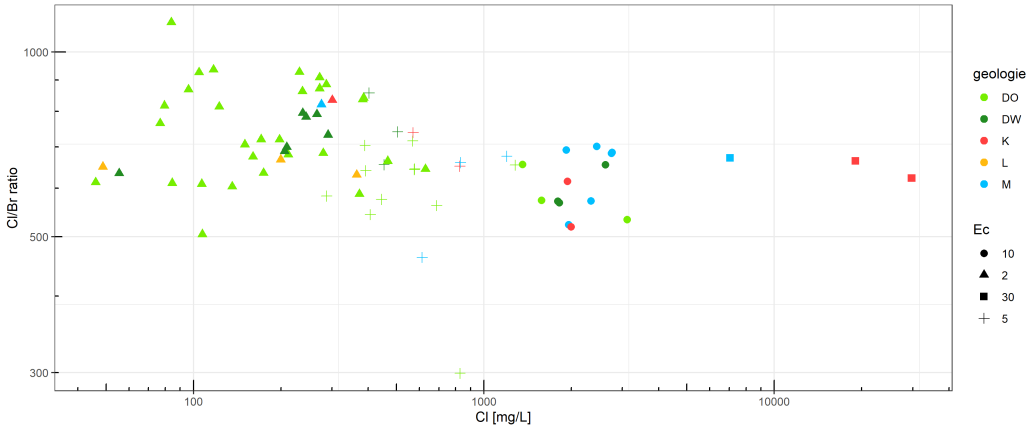

Figure A.6: Cl/Br ratio of the samples collected in 2021.

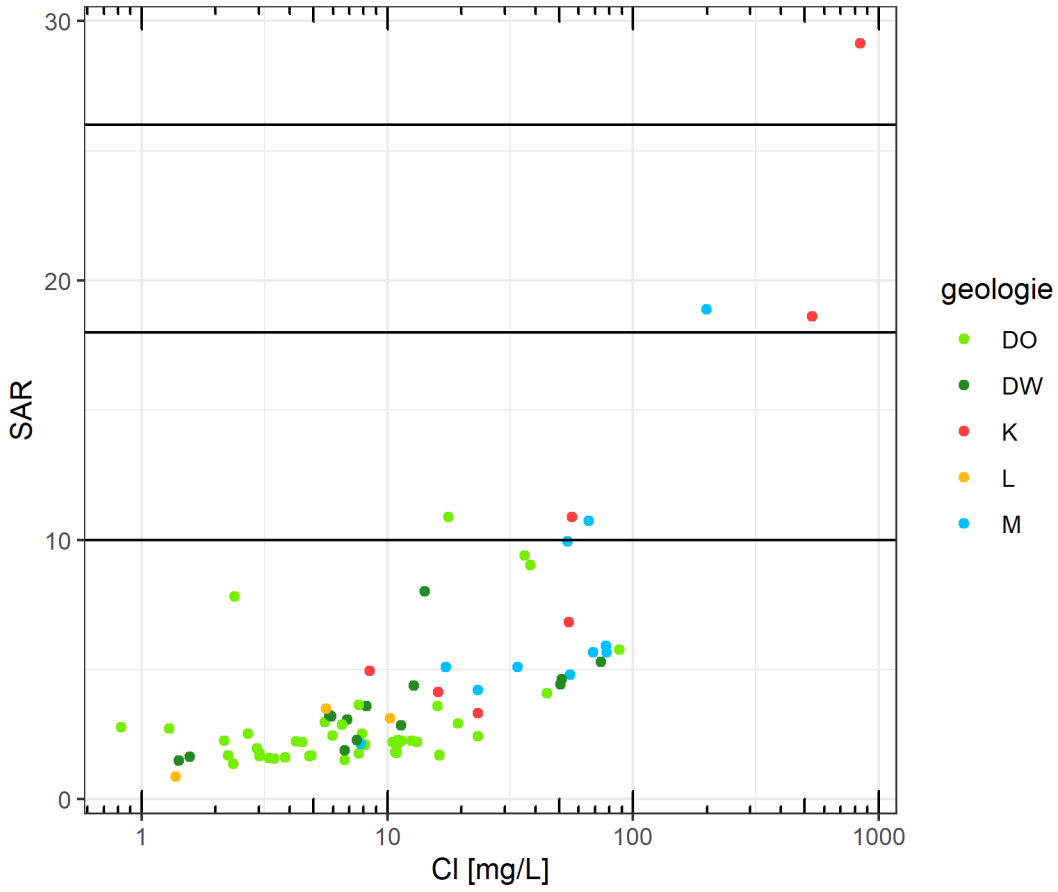

Figure A.7: Sodium Absortion Ratio (SAR) plotted against the Cl concentration, as indication for irrigation suitability: SAR< 10 "Excellent", 10-18 "Good", 18-26 "Doubtful" SAR>26 "Poor".

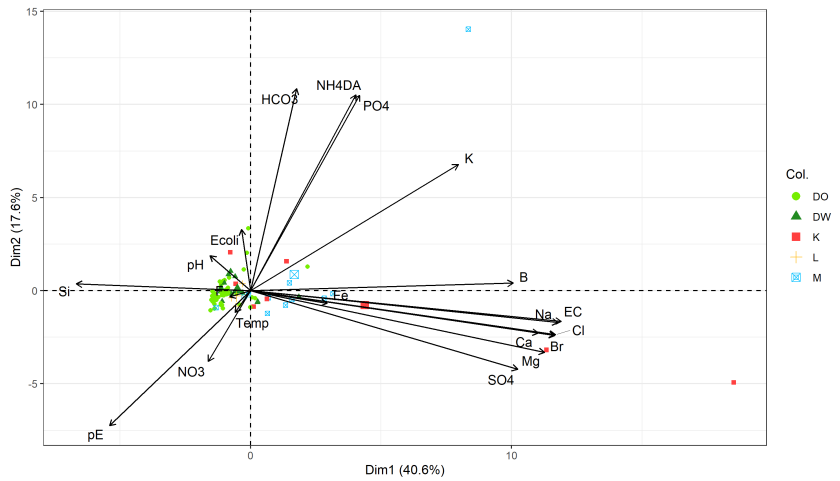

Figure A.8: PCA result for the groundwater samples of 2021.

Bibliography

Abtmaier, D. F. (1978). *Groundwaterinvestigation - curacao.*

Adshead, D., Fuldauer, L., Thacker, S., Hickford, A., Rouhet, G., Muller, W., & Hall, N. R., J.W. (2018). Evidence-based infrastructure: Curacao. national infrastructure systems modelling to support sustainable and resilient infrastructure development. *United Nations Office for Project Services, Copenhagen, Denmark.*.

Amanah, T., Putranto, T., & Helmi, M. (2019, 04). Application of cluster analysis and principal component analysis for assessment of groundwater quality—a study in semarang, central java, indonesia. *IOP Conference Series: Earth and Environmental Science*, *248*, 012063. doi: 10.1088/1755-1315/248/1/012063

Appelo, T., & Postma, D. (2005, 01). Geochemistry, ground water and pollution. *Geochemistry, Groundwater and Pollution, Second Edition*. doi: 10.1201/9781439833544

Aqualectra. (n.d.). *Rates.* Retrieved from `https://www.aqualectra.com/rates/` (accessed: 29-03-2021)

Beets, D. (1977). *Cretaceous and early tertiary of curaçao.*

Björklund, M. (2019, 08). Be careful with your principal components. *Evolution*, *73*. doi: 10.1111/evo.13835

department of Curacao, M. (n.d.). *Climate.* Retrieved from `https://meteo.cw/climate.php?Lang=Eng&St=TNCC&Sws=R11` (accessed: 24-09-2021)

de Vries, A. (2000). The semi-arid environment of curaçao: a geochemical soil survey. *Netherlands Journal of Geosciences - Geologie en Mijnbouw*, *79*(4), 479–494. doi: 10.1017/S0016774600021971

Erdogan, E. (2021). *The terrestrial consequences of poor wastewater management in curacao* (Unpublished doctoral dissertation).

Estep, A., Sandin, S., & Vermeij, M. (2017). *The state of curaçao's coral reefs.* Waitt Institute.

Grontmij, & Sogreah. (1968). Water and land resources development plan for the island of aruba, bonaire and curacao.

Güler, C., Thyne, G., Mccray, J., & Turner, A. (2002, 08). Evaluation of graphical and multivariate statistical methods for classification of water chemistry data. *Hydrogeology Journal*, *10*, 455-474. doi: 10.1007/s10040-002-0196-6

Jager, C. (2019). *CuraÇao environmental statistics compendium 2017.* Central Bureau of Statistics.

Kura, n., Ramli, M., Ibrahim, s., Aris, A., & Mustapha, A. (2013, 05). Evaluation of factors influencing the groundwater chemistry in a small tropical island of malaysia. *International journal of environmental research and public health*, *10*, 1861-1881;. doi: 10.3390/ijerph10051861

Labs, H. (2018). *What is a piper diagram for water chemistry analysis and how to create one?* Retrieved from `https://hatarilabs.com/ih-en/what-is-a-piper-diagram-and-how-to-create-one?` (accessed: 15-02-2022)

Louws, R. J., Vriend, S. P., & Frapporti, G. (1997). De grondwaterkwaliteit van curacao. *H20*, *30*(26), 4.

Martis, A., Van Oldenborgh, G. J., & Burgers, G. (2002, August). Predicting rainfall in the Dutch Caribbean - more than El Niño? *International Journal of Climatology*, *22*(10), 1219-1234. doi: 10.1002/joc.779

Molengraaf, G. (1929, 06). Geologie en geohydrologie van het eiland curaçao.

Naily, W., & Sudaryanto. (2018, 02). Cl/br ratio to determine groundwater quality. *IOP Conference Series: Earth and Environmental Science*, *118*, 012020. doi: 10.1088/1755-1315/118/1/012020

Ouyang, Y. (2005, 08). Evaluation of river water quality monitoring stations by principal component analysis. *Water research*, *39*, 2621-35. doi: 10.1016/j.watres.2005.04.024

Park, Y., Lee, K. J., J., & Song, S. (2012, 06). National scale evaluation of groundwater chemistry in korea coastal aquifers: Evidences of seawater intrusion. , *66*, 707-718.

Pathak, M. (2018). *Hierarchical clustering in r.* Retrieved from `https://www.datacamp.com/tutorial/hierarchical-clustering-R` (accessed: 20-02-2022)

Robertson, W. (2021). Septic system impacts on ground-

water quality. *Groundwater Project, Guelph, Ontario, Canada*. doi: 978-1-77470-004-4

Sarker, M., Hermans, T., Van Camp, M., Hossain, D., Islam, M., Ahmed, N., ... Walraevens, K. (2022). Identifying the major hydrogeochemical factors governing groundwater chemistry in the coastal aquifers of southwest bangladesh using statistical analysis. *Hydrology*, *9*(2). Retrieved from https://www.mdpi.com/2306-5338/9/2/20 doi: 10.3390/hydrology9020020

STHDA. (n.d.). *Factoextra r package: Easy multivariate data analyses and elegant visualization*. Retrieved from http://www.sthda.com/english/wiki/factoextra-r-package-easy-multivariate-data-analyses-and-elegant-visualization (accessed: 20-02-2022)

Tasan, M., Demir, Y., & Tasa, S. (2021). Groundwater quality assessment using principal component analysis and hierarchical cluster analysis in alaçam, turkey. *Water Supply*, *0*(0). doi: 10.2166/ws.2021.390

Tuddameri, V., Honnungar, V., & Hernandez, E. (2014). Assessment of groundwater water quality in central and southern gulf coast aquifer, tx using principal component analysis. *Environ Earth Sci*(71), 2653–2671. doi: https://doi.org/10.1007/s12665-013-2896-8

Van Buurt, G. (2018). Water conservation in curaçao; using traditional earthen dams. Retrieved from https://www.dcbd.nl/sites/default/files/documents/vanBuurt-Water%20conservation%20in%20Cura%C3%A7ao%20-%20illustrated.pdf

Van Sambeek, M., Eggenkamp, H., & Vissers, M. (2000). The groundwater quality of aruba, bonaire and curaçao: a hydrogeochemical study. *Netherlands Journal of Geosciences - Geologie en Mijnbouw*, *79*(4), 459–466. doi: 10.1017/S0016774600021958

Vermeij, J. A. (2019). *Caribbean research: a multidisciplinary approach*.

Waitt. (2016). *Economic valuation of curaçao's marine resources*. Waitt Institutes.

Yu, V. B. B. O. M. V. d. V. C., L., & Broers, H. (2018, 01). Groundwater impacts on surface water quality and nutrient loads in lowland polder catchments: Monitoring the greater amsterdam area. *Hydrology and Earth System Sciences*, *22*. doi: 10.5194/hess-22-487-2018

Zach. (2020). *K-means clustering in r: Step-by-step example*. Retrieved from https://meteo.cw/climate.php/Lang=Eng&St=TNCC&Sws=R11 (accessed: 20-02-2022)